Constraining the Age and Source Area of the Molveno landslide Deposits in the Brenta Group, Trentino Dolomites (Italy)

Author(s):
von Wartburg, Jonas; Ivy-Ochs, Susan; Aaron, Jordan; Martin, Silvana; Leith, Kerry; Rigo, Manuel; Vockenhuber, Christof; Campedel, Paolo; Viganò, Alfio

Publication date:
2020-06-05

Permanent link:
https://doi.org/10.3929/ethz-b-000423495

Originally published in:
Frontiers in Earth Science 8, https://doi.org/10.3389/feart.2020.00164

frontiers in Earth Science

ORIGINAL RESEARCH
published: 05 June 2020
doi: 10.3389/feart.2020.00164

Constraining the Age and Source Area of the Molveno landslide Deposits in the Brenta Group, Trentino Dolomites (Italy)

Jonas von Wartburg[1], Susan Ivy-Ochs[1,2], Jordan Aaron[1], Silvana Martin[3], Kerry Leith[1], Manuel Rigo[3], Christof Vockenhuber[2], Paolo Campedel[4] and Alfio Viganò[4]*

[1] Department of Earth Sciences, ETH Zürich, Zurich, Switzerland, [2] Laboratory of Ion Beam Physics, ETH Zürich, Zurich, Switzerland, [3] Dipartimento di Geoscienze, Università di Padova, Padua, Italy, [4] Servizio Geologico della Provincia Autonoma di Trento, Trento, Italy

Rock avalanches are low frequency natural hazards that can alter landscape morphology, and constraining the timing, volume and emplacement dynamics of pre-historic rock avalanches is crucial for understanding the hazards posed by these events. Here we perform cosmogenic nuclide dating, topographic reconstruction and runout modeling of the Molveno rock avalanche, located north of Lake Garda in the Province of Trento, Italy. The unique morphology of the deposits, which features numerous large scarps and prominent lineaments, have previously led researchers to interpret the Molveno rock avalanche as being the result of multiple events. Our results show that the Molveno rock avalanche had a volume of approximately 600 Mm^3, and failed from a prominent niche located on Monte Soran. ^{36}Cl cosmogenic nuclide dating results shows that the deposits were emplaced as a single event approximately 4.8 ± 0.5 ka, and suggests that the unique deposit morphology is due to the emplacement processes acting during and soon after failure. Numerical runout modeling shows that this morphology could have resulted from a combination of runup and extensional spreading of the debris along the complex valley floor topography. The ages we determined for this event are coincident with the nearby Marocca Principale rock avalanche (5.3 ± 0.9 ka), which may suggest a common trigger. Our results have important implications for interpreting the morphology of rock avalanche deposits, and contribute to the evolving understanding of rock avalanche processes in the Alps.

Keywords: rock avalanche, cosmogenic ^{36}Cl exposure dating, runout modeling, European Alps, geomorphic mapping

OPEN ACCESS

Edited by:
O. Adrian Pfiffner, University of Bern, Switzerland

Reviewed by:
Regis Braucher, UMR 7330 Centre Européen de Recherche et d'Enseignement de Géosciences de l'Environnement (CEREGE), France
Jeff Moore, University of Utah, United States

****Correspondence:***
Jordan Aaron
jordan.aaron@erdw.ethz.ch

Specialty section:
This article was submitted to Structural Geology and Tectonics, a section of the journal Frontiers in Earth Science

Received: *19 March 2020*
Accepted: *29 April 2020*
Published: *05 June 2020*

Citation:
von Wartburg J, Ivy-Ochs S, Aaron J, Martin S, Leith K, Rigo M, Vockenhuber C, Campedel P and Viganò A (2020) Constraining the Age and Source Area of the Molveno landslide Deposits in the Brenta Group, Trentino Dolomites (Italy). Front. Earth Sci. 8:164. doi: 10.3389/feart.2020.00164

INTRODUCTION

Large rock avalanches are rare mass movements that can dramatically alter landscape morphology. Many rock avalanches have filled valleys and created landslide dammed lakes, and these catastrophic events can be a significant hazard to people and infrastructure located in the potential runout zone (Schwinner, 1912; Heim, 1932; Abele, 1974; Hovius et al., 1997; Korup and Tweed, 2007; Fort et al., 2009; Loew et al., 2017). Detailed studies of pre-historic landslides are important

to understand the risk posed by these natural hazards, and understand post-glacial slope dynamics, landscape evolution, and paleoseismicity (Hovius et al., 1997; Hungr et al., 1999; Korup and Clague, 2009; Huggel et al., 2013; Grämiger et al., 2016; Ivy-Ochs et al., 2017a; Kremer et al., 2020; Singeisen et al., 2020). This requires knowledge of the volume, source area location and runout characteristics of these events, and inaccurate interpretations of these features can lead to misleading conclusions regarding rock avalanche hazard and mechanisms.

Rock avalanches are extremely rapid flows of fragmented rock that initiate as large slope failures (Hungr et al., 2014). Many rock avalanche deposits exhibit distinctive landforms, including longitudinal ridges, internal shear planes, and compressional and extensional features (Strom, 2006; Dufresne and Davies, 2009). Additionally, a characteristic stratigraphy, composed of a basal mixed zone, overlain by a highly fragmented body facies, and topped by a boulder carapace, is often observed in rock avalanche deposits (e.g., Dunning, 2004; Dufresne and Davies, 2009; Weidinger et al., 2014; Dufresne et al., 2016).

Dating of pre-historic events provides insights into rock avalanche triggering process, and facilitates comparisons to other dated landslides in the Alps. This helps to understand the temporal distribution of large mass movements during the Holocene and late Pleistocene (Prager et al., 2008; McColl, 2012), and to temporally relate the events with potential triggers and causes, such as earthquakes or climatic conditions (Ivy-Ochs et al., 2017b). Before many rock avalanches were dated, it was generally thought that they occurred within a few millennia after deglaciation, i.e., 18,000 years ago (Heim, 1932; Abele, 1974). This hypothesis implied that glacier debuttressing was a primary trigger of rock slope failure, an interpretation that has been called into question (McColl, 2012). More recently, surface exposure dating has revealed that many rock avalanches in the Alps occurred during the middle and late Holocene (Bigot-Cormier et al., 2005; Hippolyte et al., 2006; Cossart et al., 2008; Prager et al., 2008; Hippolyte et al., 2009; Le Roux et al., 2009; Ivy-Ochs et al., 2017a). Large landslides in the Alps show three periods of enhanced slope activity: 10–9, 5–3, and 2–1 ka, the latter especially for the Southern Alps (Prager et al., 2008; Zerathe et al., 2014; Ivy-Ochs et al., 2017a). Thus, most large landslides happened during the Holocene, at least 6000 years after the retreat of glaciers from the affected valleys, and many of them in quite recent time (Ivy-Ochs et al., 2017a).

The study of pre-historic rock avalanches has revealed that oversteepened valley flanks, and reduced support by glaciers, is one of several important causes, but not necessarily a trigger of rock avalanches (McColl, 2012; Grämiger et al., 2017). It is generally believed that a changing climate has an influence on landslide hazard, for example due to change in precipitation, and/or melting permafrost (Kellerer-Pirklbauer et al., 2012; McColl, 2012; Stoffel and Huggel, 2012; Huggel et al., 2013; Zerathe et al., 2014; Coe et al., 2018). In the Holocene, the climate became warmer and wetter, which may explain the three periods of enhanced slope activity described above (Prager et al., 2008; Ivy-Ochs et al., 2017a). However, for pre-historic rock avalanches it is challenging to detect climatic influence, due to their relatively low frequency (Huggel et al., 2013). Earthquake triggering has also been proposed to explain temporal clustering of pre-historic rock avalanches (McColl, 2012; Grämiger et al., 2016; Knapp et al., 2018; Köpfli et al., 2018).

In addition to providing important information about rock avalanche triggering mechanisms, the age and volume of large events are an important contribution to understanding the magnitude frequency relationship of rare events (Hovius et al., 1997), which are often missing in historic event cadasters (Hungr et al., 1999). However, if the deposits of a pre-historic event are mistakenly interpreted to be formed from multiple events, then the resulting magnitude-frequency relationship would be highly inaccurate. Finally, understanding the emplacement characteristics of past events contributes to understanding and predicting the mechanisms that govern rock avalanche mobility (e.g., Aaron and McDougall, 2019).

Thus, constraining the age, volume and emplacement dynamics of pre-historic case histories provides important insights into rock avalanche hazard and mechanisms. The aim of this study is to determine these parameters for the Molveno rock avalanche. The geomorphic characteristics of this site, which include large internal scarps, have led to a number of incompatible interpretations regarding the source location, age and number of events that make up the deposit. This makes it difficult to place the Molveno rock avalanche in a regional context and to interpret how this event contributes to the evolving understanding of rock avalanche processes in the Alps. To address these uncertainties, we perform detailed geomorphic mapping, cosmogenic nuclide dating, topographic reconstruction, and 3D runout analysis.

STUDY AREA

The study area, shown in **Figure 1**, is located in the lower Sarca Valley, north of Lake Garda in the Province of Trento, Italy. Molveno belongs to a cluster of large landslides (**Figure 1**). The oldest of these is Marocca Principale (5.3 $\pm$ 0.9 ka), located approximately 10 km away from Molveno (Ivy-Ochs et al., 2017a). Another nearby deposit is Tovel (<20 km away from Molveno), which is composed of at least two events (Ferretti and Borsato, 2004). Lavini di Marco (3.0 $\pm$ 0.4 ka) dates to the late Holocene (Martin et al., 2014). The other five dated landslides in Trentino are of historic age (Ivy-Ochs et al., 2017a).

Deposits of the Molveno rock avalanche(s) are situated in a NNE-SSW trending valley which is parallel to the Giudicarie fault system (Castellarin et al., 2005a). As shown on **Figure 1**, the study area is tectonically dominated by the southern Giudicarie fold and thrust belt (Castellarin et al., 2005a, 2006; Viganò et al., 2015). The Molveno Valley is dominated by a syncline, the fold axis of which is dipping toward SSW (Castellarin et al., 2005a). The Molveno Valley has an asymmetric profile, with a steep western flank, affected by scarp-fault-surfaces, and a gently dipping eastern flank which follows the orientation of stratification (Carton, 2017). Most large aquifers, and point-springs of high to very high capacity (100 to 500 l), are related to the Triassic dolomites of the Dolomia Principale formation

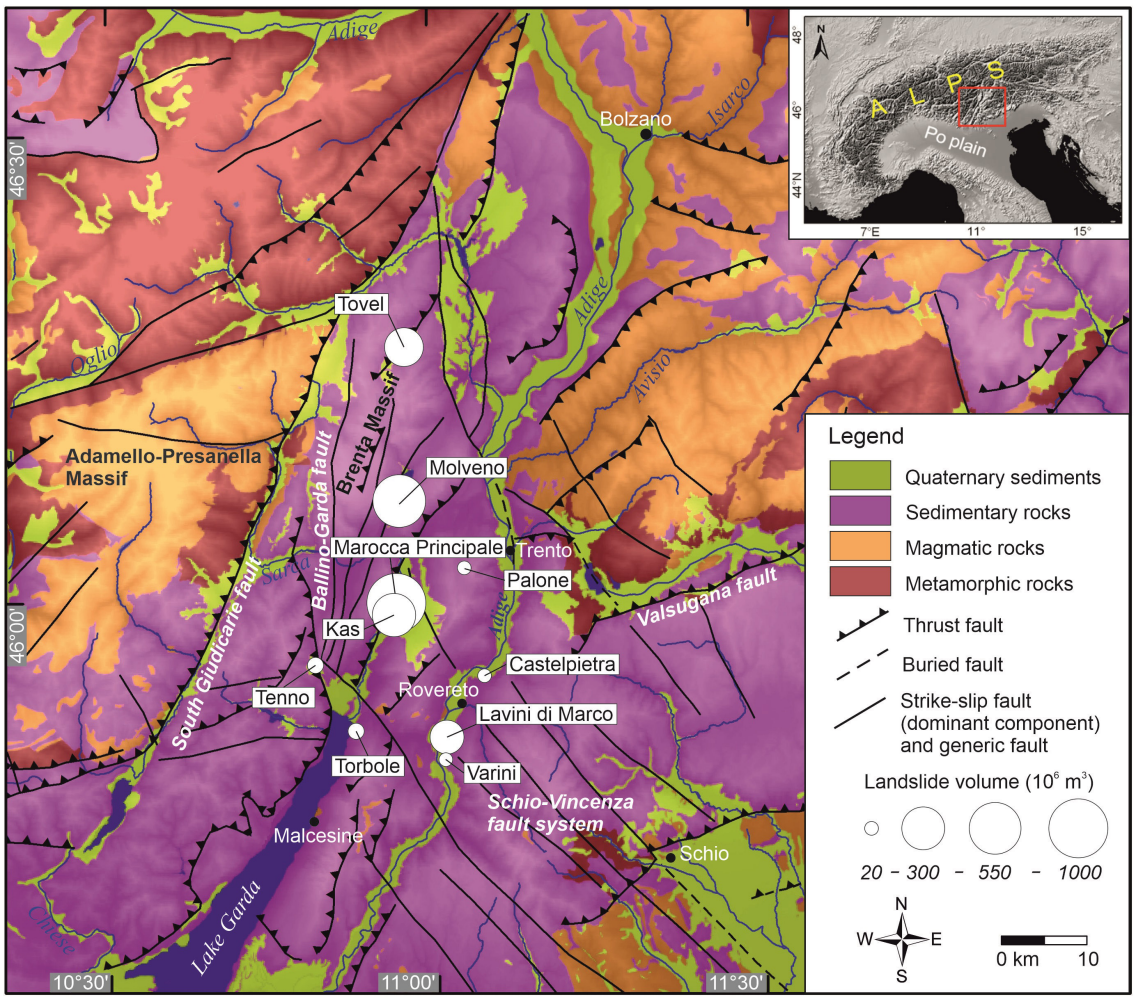

FIGURE 1 | Geological map showing rock avalanches in the province of Trento and their approximate size. Geologic data from the Geological Survey of Trento, CARG project database. Map modified from Ivy-Ochs et al. (2017a). The studied landslide is labeled as "Molveno."

and the overlaying Triassic limestones of the Calcari Grigi Group (Castellarin et al., 2005b).

The main lithologies of the study area are the typical formations of the Trentino carbonate platform, and the Molveno rock avalanche deposit consists mainly of oolitic limestone (Castellarin et al., 2005b). The Rotzo formation, which forms the base of the proposed source area, is known to have marly interbeds (Castellarin et al., 2005a).

Previous Work

The location of the source area, as well as the number of events that make up the Molveno rock avalanche deposits, has been debated by many authors (Lepsius, 1878; Damian, 1890; Trener, 1906; Schwinner, 1912; Trevisan, 1939; Marchesoni, 1954; Marchesoni, 1958; Fuganti, 1969; Abele, 1974; Chinaglia, 1992; Carton, 2017). Lepsius (1878) stated that the rock avalanche initiated on Monte Gazza, located on the western valley flank (**Figure 2C**). In contrast, Damian (1890) suggested that the rock avalanche initiated from Monte Soran (**Figures 2C**, **3A**). Schwinner (1912) also suggested the source area was located on Monte Soran, and was the first to estimate the volume of the landslide, which he estimated to be between 300 and 500 Mm^3. Fuganti (1969) locates the source area, in contrast to Damian (1890) and Schwinner (1912), and in line with Lepsius (1878), at the eastern side of the valley at Monte Gazza (**Figures 2**, **3C**), south of Pian delle Gaorne, in a prominent niche (**Figure 3D**). Chinaglia (1992) estimated the volume of the deposit to be 750 Mm^3, and suggested it was composed of four different landslides. One key aspect of this interpretation is that the prominent scarps featured in the debris (discussed in the following section) have been used as evidence that the deposits formed during several different events.

Radiocarbon dates associated with the Molveno rock avalanche have been reported by Marchesoni (1954, 1958). Marchesoni (1958) dated several logs obtained from Lago di Molveno when it was emptied for a hydropower project in 1951/52, and determined an age of 2908 ± 153 ^{14}C year BP (3441–2752 cal BP). In this work, several logs were sampled from

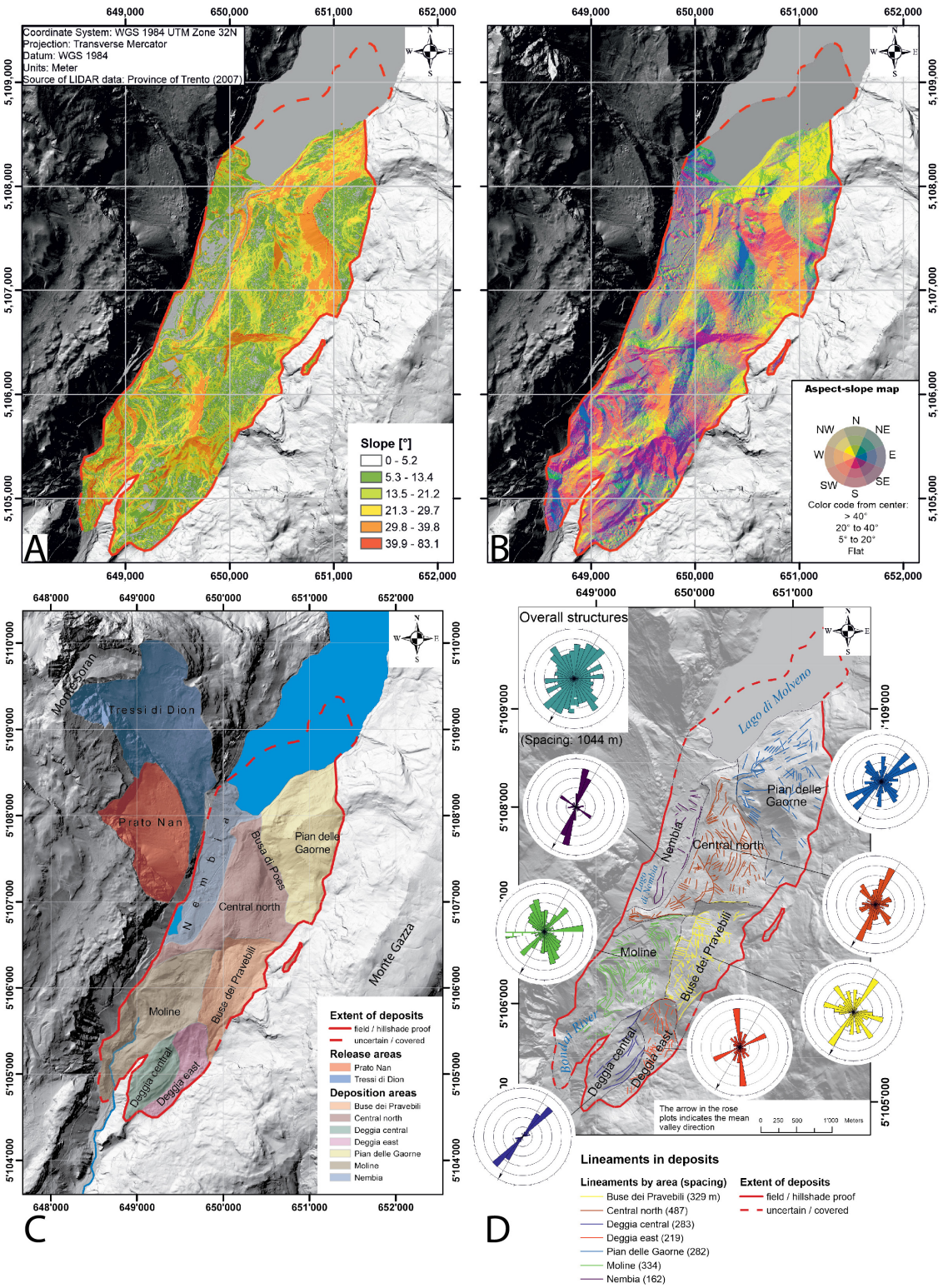

FIGURE 2 | (A) Slope map of the Molveno deposits. **(B)** Aspect map of the deposits. **(C)** Landslide regions. Deposition and release area. The red line encircles the mapped landslide deposits. The proposed release area is in the Northwest, it comprises Prato Nan and Tressi di Dion. **(D)** Lineament map of deposit structures. For each of the landslide areas lineaments were drawn on the aspect-slope map and hillshade. The lineaments are plotted length normalized as rose plots, i.e., the direction with greatest cumulative length is the longest rosette branch, and so on. A bin size of 10° was chosen. The concentric circles on each plot correspond to lineament length, with spacing the circles indicated on the legend. Map coordinate system: WGS 1984 UTM Zone 32N.

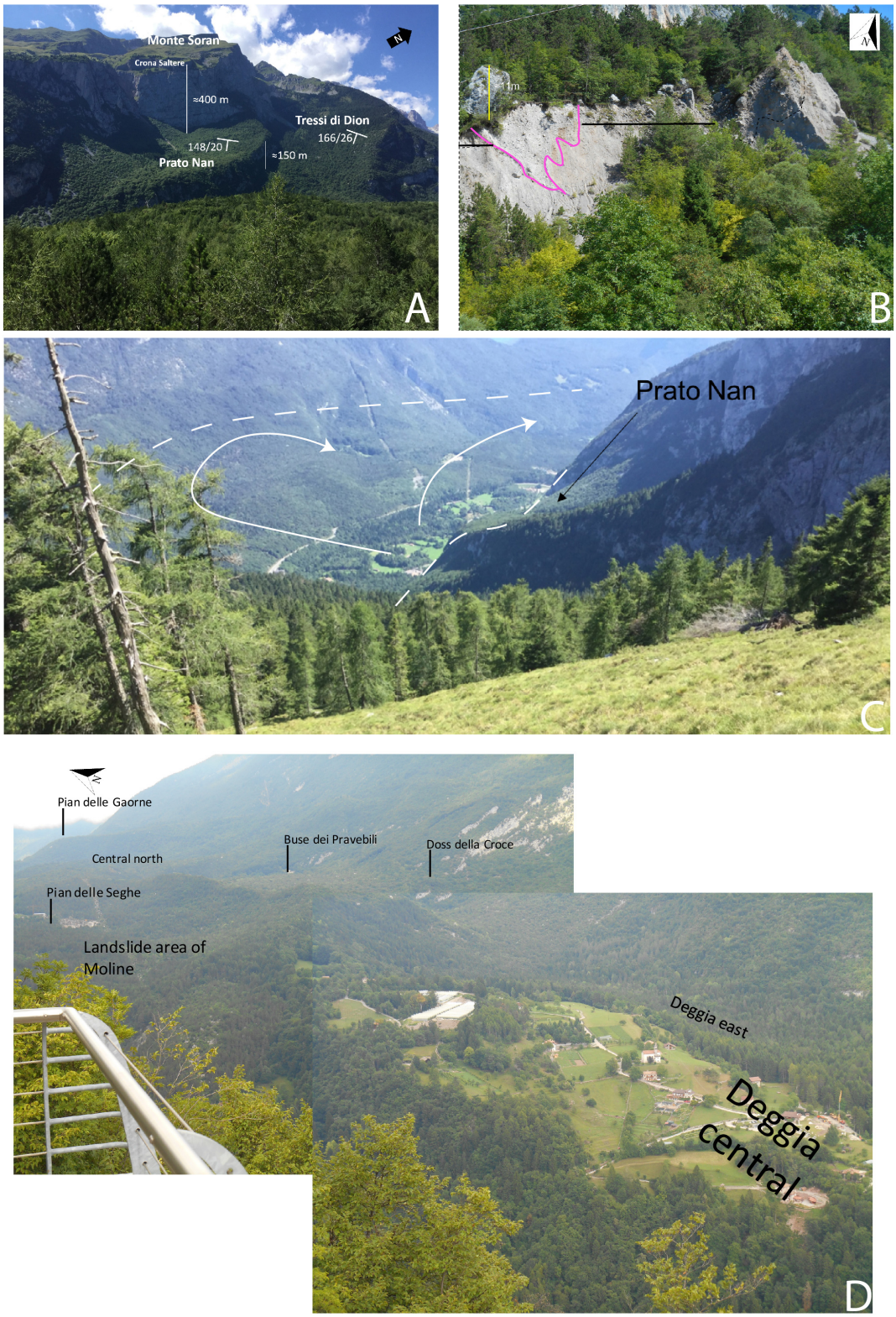

FIGURE 3 | (A) Image of rupture surface, showing both Prato Nan, and Tressi di Dion. **(B)** Outcrop of landslide deposits at Moline. Typical example of a carapace (large boulders on top) and strongly comminuted material inside the deposits. The carapace layer is indicated with a black line. The purple line shows a wedge-shaped pattern of coarser looking material. The boulder on top is around 11 m high (Photo: S. Ivy-Ochs). **(C)** Overview of the landslide looking from Tressi di Dion toward Pian delle Gaorne. **(D)** Overview of deposit zones.

a drowned forest, which was located on top of the deposits, and also a buried log (32 m below ground) from the construction site at the plain of Nembia, shown on **Figure 2C** (Marchesoni, 1954, 1958). The reported date is a composite date based on analysis of a single sample made up of several wood fragments, therefore it must be viewed with caution. The suggested age could also be constrained by other items used by human settlers, found further north on the lake floor, which are from into the Iron Age (Marchesoni, 1954).

GEOMORPHOLOGICAL ANALYSIS

We have performed geomorphic mapping of the site in order to document surficial features of the source zone and deposit. These provide field evidence to help understand the failure and emplacement of the Molveno rock avalanche. Our mapping included measurements of several geometric characteristics (such as planar area) of the source and deposit zone, a subdivision of the deposit into distinct geomorphic areas, and mapping of the location and extent of scarps, ridges and lineaments. This was done by manually digitizing all these features on a hillshade projection of available LiDAR data.

As will be summarized further in the section entitled "Reconstruction of pre-failure topography and volume analysis," we tested whether the emplacement characteristics of the event could be explained with a source area located on Monte Soran. This source location has a total planar area of approximately 2.74 Mm^2 and can be subdivided into a northern niche called Tressi di Dion that has an area of 1.74 Mm^2 and a southern niche called Prato Nan, covering 1.00 Mm^2. These source niches are shown on **Figures 2**, **3A,C**. The crown of the scarp has a total length of about 5000 m. The source reaches from 2360 m a.s.l. at the peak of Monte Soran down to around 900 m a.s.l., where an approximately 100 m high bedrock step separates it from the plain of Nembia. The slope of Tressi di Dion, with an average of 26°, is steeper than the slope of Prato Nan with 20°. Throughout the whole length of Prato Nan, very large boulders of up to 25 m diameter are found, which are interpreted as rock avalanche deposits (Castellarin et al., 2005a).

The deposition area of the landslide, shown on **Figures 3B,D**, is estimated to cover an area of 5.7 to 6.4 Mm^2. Between 0.5 and 1.2 Mm^2 are submerged in Lago di Molveno, based on mapping by Marchesoni (1954). The deposits are angular, well graded gravel with many large boulders, mainly on top, and many cobbles and blocks within the deposits.

As shown on **Figure 2C**, the deposit area is divided into seven separate areas, discussed below from North to South:

- Nembia, which is characterized by its flatness, large boulders and hillocks, and is surrounded by meadows. The flat areas are composed of lake sediments underlain by large boulders.
- Central North, which reaches from Lago di Molveno down to the ridge below the plain of Nembia. This region is defined by prominent trenches and depressions, and features numerous lineaments (**Figure 2D**). Large boulders cover the surface.
- Pian delle Gaorne, which is an elevated semicircular platform-like landform, located 200 m above Lago di Molveno. The entire plain is covered by large boulders and finer grained landslide debris. Most boulders are in the range of 5 to 15 m in diameter.
- Buse dei Pravebili, which is a topographic depression separated from the Central North zone by a 50 m high, 600 m long scarp. This area is partly covered by an alluvial fan, and features many large boulders.
- Moline, which contains a small settlement and limestone quarry. This area has been heavily modified by anthropogenic activities. An outcrop showing the sedimentology of the landslide deposits can be seen in the eroded landslide deposits above Moline (**Figure 3B**). A boulder carapace, consisting of boulders up to 11 m in diameter, can be observed at the surface (e.g., Dunning, 2004; Dufresne and Davies, 2009; Weidinger et al., 2014). However, large boulders are also found in the body facies. Within the deposits, slump structures can be seen (**Figure 3B** below the large boulder). Strongly comminuted material underlies the carapace layer. Below the 11 m high boulder, a wedge of sediment bound by an internal sliding plane is visible (marked in purple in **Figure 3B**).
- Deggia East, which is a forested, hummocky area, with hummocks that are on the order of 20 to 50 m in diameter. It is separated from Buse dei Pravebili by a 150 m high, 35° steep major scarp (**Figures 2A,B**).
- Deggia central, which is a settlement on a bedrock high at the centre of the valley. Based on bedrock outcrops and a construction site, the thickness of the landslide deposits here is estimated to be less than 10 m.

The deposit features numerous scarps and ridges (**Figures 2A,B**). These are especially prominent between the Central North and Buse dei Pravebili regions, as well as in Moline (**Figures 2A,B**). These features have been interpreted as evidence that the deposit is composed of multiple events (Chinaglia, 1992), and it was previously unknown if these features formed during or after the emplacement of the rock avalanche(s).

Another striking feature of the deposit is the presence of numerous lineaments within the debris. As shown on **Figure 2D**, the lineaments have two dominant orientations, one parallel to the presumed direction of motion and the other perpendicular. These features provide important dynamic information as they either align with the local direction of motion, or provide evidence for compression and extension during runout (Strom, 2006; Dufresne and Davies, 2009). These features are numerous in all deposition sectors, except for Nembia. The orientation of the two sets of lineaments is consistent in Nembia, Central North, and Buse dei Pravebili. Similarly, the orientations are consistent in Deggia East and Pian delle Gaorne. These observations are discussed further in section "Runout analysis," after the

results of the cosmogenic nuclide exposure dating and runout analysis are presented.

COSMOGENIC NUCLIDE SURFACE EXPOSURE DATING

Constraining the age of the landslide is an important contribution to understanding the post-glacial dynamics, and to be able to correlate the timing of the landslide with possible triggers e.g., seismic crises or climatic conditions. Additionally, dating of boulders in the different landslide areas provides a direct means of establishing the number of landslides that the deposit is composed of. Since the deposit is composed of limestone, cosmogenic ^{36}Cl was used for dating. Cosmogenic nuclides are produced within minerals of rock surfaces exposed to cosmic rays. Measuring the concentration of the cosmogenic nuclide allows calculation of the time elapsed since boulder deposition (Ivy-Ochs and Kober, 2008).

During fieldwork, numerous boulders were examined for suitability for dating, using the criteria given by Ivy-Ochs and Kober (2008). The main considerations were that the block be large, weathering-resistant, and stand locally high in the landscape. Two sampling campaigns were conducted: The first campaign was in 2009 when three samples were collected, MO1 to MO3; two of these were successfully dated (for MO2, during measurement the ^{36}S counts were too high and measurement was stopped). In the second sampling campaign, in 2017, eight samples (MO4–MO11) were taken and all dated. Photos of select boulders are shown in **Figure 4**, and the locations of the samples are shown in **Figure 5**.

We followed the sample preparation procedure using isotope dilution as given by Ivy-Ochs et al. (2004). Rock samples were crushed to <0.4 mm, leached with water and dilute HNO_3, then dissolved completely with HNO_3 after addition of ^{35}Cl carrier. Sample AgCl was isolated and purified in a series of precipitation and dissolution steps. To avoid ^{36}S interferences during accelerator mass spectrometer (AMS) measurements, sulfur was removed through precipitation of $BaSO_4$ after addition of $Ba(NO_3)_2$. Measurement of both ^{37}Cl/^{35}Cl as well as ^{36}Cl/Cl ratios is with the 6 MV tandem accelerator at Ion Beam Physics, ETH Zurich. ^{36}Cl/Cl ratios were measured against the ETH internal standard K382/4N with a value of ^{36}Cl/Cl = 17.36×10^{-12} which has been calibrated to international AMS standards (Vockenhuber et al., 2019). Sample ratios were corrected for a blank value of 3.2×10^{-15}. Elemental concentrations (**Table 1**) as required for age calculations were determined commercially at Actlabs (Toronto, Canada).

Calculation of the ^{36}Cl exposure ages, applying all corrections, was conducted using an the in-house MATLAB© code developed at Ion Beam Physics ETH Zurich. A density of 2.4 g/cm^3 was used, and production rates were scaled to the boulder locations using the time dependent scaling model (Lm; Balco et al., 2008). Implemented equations, constants and production rates are given by Alfimov and Ivy-Ochs (2009). We used the calcium spallation production rate of 48.8 ± 3.4 ^{36}Cl atoms g_{Ca}^{-1} year^{-1} and a contribution due to muon capture on Ca of 9.6% at the rock surface (Stone et al., 1996). For calculation of production of ^{36}Cl through low-energy neutron capture, a value of 760 ± 150 neutrons g_{air}^{-1} year^{-1} was used (Alfimov and Ivy-Ochs, 2009). These values agree well with the ^{36}Cl production rates recently published by Marrero et al. (2016). Final age uncertainties (**Table 2** and **Figure 5**) include both analytical (one sigma) and production rate uncertainties. All production mechanisms are included in the age calculations. Shielding corrections were determined using ArcGIS from the digital terrain data.

The dating results show a cluster of boulder ages between 4.1 ± 0.3 to 5.5 ± 0.4 ka (**Table 2**), and a smaller cluster comprised of two dates, 2.1 ± 0.3 and 2.4 ± 0.2 ka. There is a clear spatial pattern for these ages. The two younger ages are from two closely situated boulders at Nembia (**Figure 5**). The other eight ages are from boulders found all across the Molveno deposits. The sampled boulders lie in the following areas (**Figure 5**): On Pian delle Gaorne three samples (MO4, 5, 6) whose ages range from 4.7 ± 0.3 to 5.1 ± 0.3 ka; In Central North, two samples date to 5.0 ± 0.6 ka (MO9), and 5.5 ± 0.4 ka (MO1); On Buse dei Pravebili, three samples (MO3, 7, 8) with ages between 4.1 ± 0.3 ka, and 4.9 ± 0.3 ka were determined. There is some scatter to these dates, however, in all three geographical areas at least one sample lies within the range of 4.9 ± 0.3 and 5.1 ± 0.4 ka. We therefore assume that all sampled geomorphological areas (**Figure 5**) are part of the same event with an average age of 4.8 ± 0.5 ka. All ages are included in the average except for MO10 and MO11 from Nembia.

Nembia (**Figure 2C**) is a distinct area due to its notable flatness reflecting the presence of lake sediments. Large landslide boulders are much younger (2.2 ka) than the rest of the deposits. These younger ages can be due to: (1) a later detachment by a second rock slide or rock avalanche, (2) shielding from cosmic rays after the event by sediment or water, or (3) loss of the top surface of the boulder by spalling. There is a small detachment zone in the bedrock above Nembia at the southwestern margin of Prato Nan, however, the lithology of Prato Nan does not match the lithology seen in the deposits at Nembia. Therefore, we consider the second possible explanation, shielding from cosmic rays, more likely.

There is no evidence for sediment covering the sampled surfaces. But in accordance with the presence of lake sediments underlying the plain, it is conceivable that water was previously covering the boulders, and a subsequent event led to drainage of the lake. The deposits south of Nembia, which form a transverse ridge have an elevation of around 815 m a.s.l. If they would have blocked the lake, the lake level would have had a maximum level of 815 m a.s.l. water cover, which would have been at least 10 m above both blocks, as MO11 is at 792 m a.s.l., and MO10 805 m a.s.l., would have provided sufficient shielding from cosmic rays. The production rate of ^{36}Cl in limestone is less than 5% of the surface value below 3 m depth (Steinemann et al., 2020). As attenuation is density dependent, water more than 9 m in depth would have provided sufficient shielding to reduce ^{36}Cl production to less than 5% of the non-shielded value.

Below Nembia no clear evidence of a catastrophic dam breach can be found, however, Evans et al. (2011), based on a database of landslide dam breaches, show a wide variety of breach

FIGURE 4 | Examples of boulders used for surface exposure dating (**Table 1**). Written informed consent was obtained from the individuals for the publication of any potentially identifiable images or data included in this article.

morphologies, often with no clear markers of a catastrophic event. The coherence of the two boulder dates suggests that 2.2 ka may be a good approximation for the timing of the breaching event and that both blocks were covered by enough water to shield them from cosmic rays. Accordingly, 815 m a.s.l. may well represent the elevation of the lake surface between 4.8 and 2.2 ka. Importantly, no geomorphological evidence of a discontinuity between the blocky deposits at Nembia and the main Molveno rock avalanche deposits can be found.

RECONSTRUCTION OF PRE-FAILURE TOPOGRAPHY AND VOLUME ANALYSIS

The volume of the rock avalanche(s) is a key element in the landslide analysis. It is an important parameter for understanding the dynamic behavior of the landslide, i.e., reach and velocity (Scheidegger, 1973), and also a main input parameter, for magnitude frequency relationships (Hungr et al., 1999). As described above, previous authors have estimated the volume

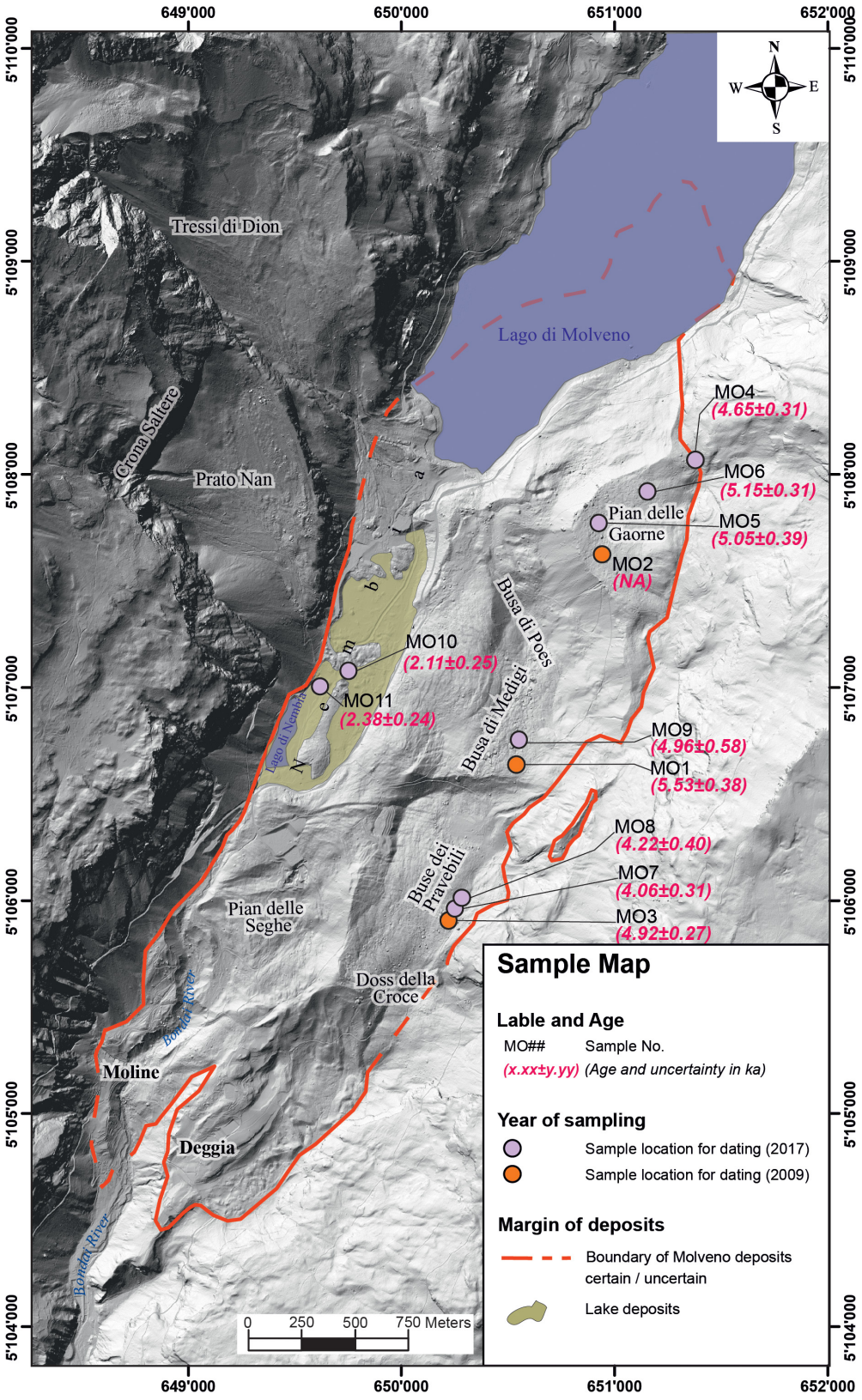

FIGURE 5 | Sample and ^{36}Cl exposure age map. All samples dated are shown in this figure (MO02 could not be dated due to too high ^{36}S counts during AMS). Coordinate system: WGS 1984 UTM Zone 32N.

TABLE 1 | Chemical composition of the samples used for cosmogenic nuclide dating.

	Sm ppm	Gd ppm	Th ppm	U ppm	Si02 w%	Al203 w%	Fe203(T) w%	MnO w%	MgO w%	CaO w%	Na20 w%	K20 w%	Ti02 w%	P205 w%
MO 1	0.1	0.1	0.1	1.5	0.12	0.11	0.05	0.010	0.27	54.95	0.01	0.01	0.010	0.02
MO 2	0.1	0.1	0.0	2.0	0.06	0.07	0.07	0.010	0.24	55.16	0.01	0.01	0.010	0.01
MO 3	0.1	0.1	0.1	2.0	0.03	0.04	0.03	0.010	0.24	55.37	0.01	0.01	0.010	0.01
MO 4	0.2	0.3	0.1	0.6	0.23	0.09	0.06	0.004	0.61	55.98	0.03	0.02	0.004	0.29
MO 5	0.3	0.3	0.5	1.1	1.40	0.73	0.40	0.006	0.77	53.74	0.04	0.23	0.036	0.03
MO 6	<0.1	0.2	<0.1	0.3	<0.01	0.10	0.06	0.003	0.40	55.77	0.05	0.02	0.001	<0.01
MO7	0.3	0.3	0.3	1.3	0.18	0.22	0.07	0.003	0.61	55.35	0.04	0.06	0.009	<0.01
MO8	0.1	0.2	<0.1	0.6	0.07	0.14	0.07	0.003	0.49	55.62	0.06	0.03	0.002	0.01
MO 9	0.1	0.2	0.1	0.7	<0.01	0.13	0.05	0.003	0.57	55.65	0.03	0.04	0.004	0.01
MO 10	<0.1	<0.1	<0.1	0.4	<0.01	0.11	0.06	0.003	0.33	55.82	0.05	0.02	0.001	0.02
MO 11	<0.1	0.1	<0.1	0.3	<0.01	0.13	0.05	0.003	0.53	55.64	0.05	0.03	0.002	0.06

The here listed chemical components are the most important ones for the production rate of ^{36}Cl, i.e., also for the dating.

TABLE 2 | Sample data. Spatial location, orientation, thickness, chlorine concentration, and calculated ages.

	Lat (°N)	Long (°E)	Elevation (m a.s.l)	Samp. Thickn. (cm)	Shielding corr	Cl (ppm)	10^6 atoms ^{36}Cl/ (*g* rock)	Exposure age (ka)
MO1	46.0967	10.9475	920	5	0.947	15.5 ± 0.2	0.238 ± 0.014	5.53 ± 0.38
MO3	46.0902	10.9432	850	2	0.960	16.5 ± 0.1	0.209 ± 0.009	4.92 ± 0.27
MO4	46.1094	10.9588	1037	4	0.962	11.7 ± 0.1	0.222 ± 0.013	4.56 ± 0.31
MO5	46.1068	10.9529	1012	3	0.980	21.1 ± 0.3	0.247 ± 0.017	5.05 ± 0.39
MO6	46.1081	10.9559	1035.9	2.5	0.966	11.5 ± 0.0	0.253 ± 0.013	5.15 ± 0.31
MO7	46.0907	10.9436	849	5	0.937	13.6 ± 0.2	0.164 ± 0.011	4.06 ± 0.31
MO8	46.0912	10.9440	842	4.5	0.967	14.0 ± 0.1	0.177 ± 0.016	4.22 ± 0.40
MO9	46.0978	10.9478	899	3	0.912	16.3 ± 0.3	0.208 ± 0.023	4.96 ± 0.58
MO10	46.1009	10.9375	802	5	0.958	14.3 ± 0.1	0.085 ± 0.010	2.11 ± 0.25
MO11	46.1002	10.9358	792	5	0.886	15.4 ± 0.2	0.088 ± 0.009	2.38 ± 0.24

Two groups of ages are distinguished. The main body (4.8 ky) and a minor body (2.2 ky), marked brown in ***Figure 5****.*

of the landslide. However, the thickness of the deposits has not been previously estimated. A comparably minor uncertainty is the extent of the landslide into the lake. The pre-failure topographic surface is also a key input for the runout modeling, described below.

To estimate the volume of the source area, we manually modified the contour lines in the source area to provide a smooth transition with surrounding terrain. In the deposit area, a seismic survey, conducted while planning of the dam (Vecchia, 1953), was used to constrain the bedrock depth at Nembia, in the southern part of Lago di Molveno and in the area of Busa di Poes (**Figure 2C**). In addition to this, we have combined LiDAR data from the Province of Trento and an assumed pre-failure river profile for the valley to the estimated pre-failure surface. The volumes of the source and the deposition area were determined by differencing the present day topography with the reconstructed pre-event topography, and removing the volume of water assumed to be contained in the lake. For this, the contour map of the lake floor, presented by Vecchia (1953), was used. The calculated volumes are shown in **Table 3** and the reconstructed topography, as well as the source and deposit thicknesses, are shown in **Figure 6**.

Based on the back-analysis of various rock avalanche case studies, Hungr and Evans (2004) estimated a typical bulking factor (ratio of deposit volume to source volume) of 25%. Our reconstruction resulted in a bulking factor of 8%, which is somewhat lower. However, our reconstructed deposit volume fits well within the ranges estimated by previous authors [300–500 Mm^3 (Schwinner, 1912) to 750 Mm^3 (Chinaglia, 1992)]. Thus, given the uncertainties inherent in reconstructing pre-event topography, our source and deposit volumes are likely reasonable approximations of the pre-event conditions.

In our topographic reconstruction, the deposit is thickest at Pian delle Gaorne (**Figure 6**). There are two potential explanations for this. (1) Pian delle Gaorne is a bedrock high, covered with landslide debris. If this is the case, then we have overestimated the thickness of deposits in this area. However, there are no bedrock outcrops which would support this hypothesis. (2) Pian delle Gaorne is composed entirely of landslide deposits which remained more intact than the rest.

TABLE 3 | Calculated volumes of the source and deposition area of the rock avalanche of Molveno.

	Volume (Mm^3)
Deposit volume	600
Source mass	550

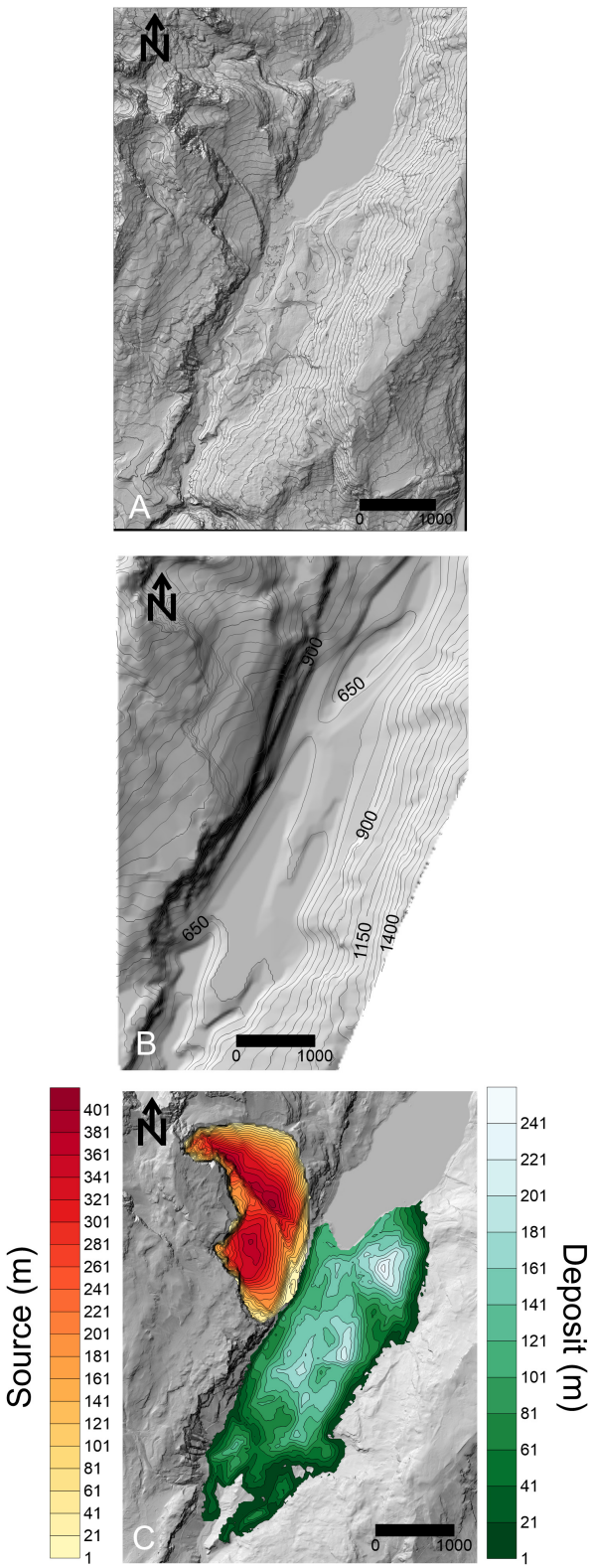

FIGURE 6 | (A) Present day topography (LiDAR data provided by province of Trento). **(B)** Reconstructed pre-failure topography. **(C)** Reconstructed source and deposit thickness, only material reconstructed above the present-day lake is shown.

That means it would have had high internal strength, however, there is also no direct evidence for this hypothesis. At the contact to the bedrock along the eastern valley side, a small ridge and a distinct depression through the whole length of the contact are visible (**Figure 2A**). This ridge and depression were interpreted to be signs for compression (e.g., Strom, 2006; Dufresne et al., 2016; Wolter et al., 2016), or run up and fall back (e.g., Evans et al., 1994).

Our estimated source volume can be used to compare the mobility of the Molveno rock avalanche to other large rock avalanches. A plot of fall height (H) divided by runout length (L) as a function of volume for the Molveno rock avalanche, as well as a large number of rock avalanche case histories assembled by Scheidegger (1973) and Li (1983) is shown in **Figure 7** (see inset for explanation of these two terms). As summarized in Heim (1932), the inclination of the line connecting the centers of mass of the source and deposit (red line on the inset of **Figure 7**) is equal to the basal friction angle, if the mass is assumed to move as a sliding block. Rock-on-rock sliding is expected to have a centre-of-mass fall height to runout length ratio of 0.6, and values lower than this indicate that additional mechanisms must reduce basal resistance (Scheidegger, 1973). The inclination of the line connecting the tip of the scarp to the toe of the deposit (H/L), approximates this angle, and is easier to measure in practice. Due to this, H/L serves as a useful empirical parameter for comparing mobility of different rock avalanches. As can be seen on **Figure 7**, the mobility of the Molveno rock avalanche was relatively low, compared to other rock avalanches of similar volume.

RUNOUT ANALYSIS

We perform semi-empirical runout modeling to simulate the impact area and deposit thicknesses, and to verify our proposed source geometry and location. For the simulations presented here, we used the depth averaged, 3D runout model Dan3D-Flex (Aaron and Hungr, 2016b). This model simulates the motion of an "equivalent fluid" over 3D terrain (Hungr, 1995). The rock avalanche is initially treated as a flexible block, able to translate, and rotate over 3D terrain. At a user specified time, the model transitions into a frictional fluid (McDougall and Hungr, 2004). The program features an open rheological kernel to calculate the basal resistance stress, and the parameters that govern the basal rheological model are calibrated. For the present analysis, we use the frictional and Voellmy rheologies, summarized in Hungr and McDougall (2009). The fluid portion of the model is a depth-averaged continuum dynamic model, incorporating an earth pressure theory similar to the classical Rankine earth pressure theory, where stresses linearly increase with depth (Savage and Hutter, 1989).

The parameters used for our best-fit model are listed in **Table 4**. **Figure 8** shows position and extent of the landslide at selected time intervals, **Figure 9** shows a number of cross sections through the results, and **Figure 10A** shows the final simulated deposit thicknesses and impact area. At t = 0 s the landslide is in its initial source niche. After 30 s the still coherent landslide mass hits the valley floor and disintegrates. At this

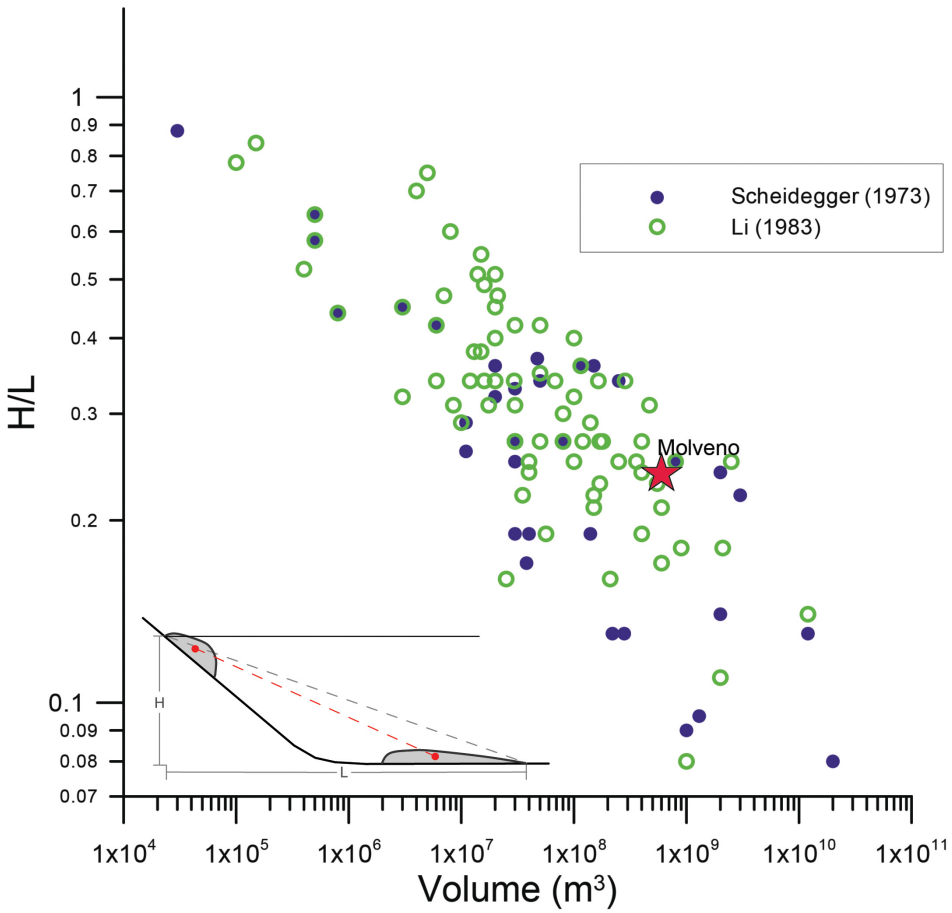

FIGURE 7 | Scheidegger-Plot (Volume vs. H/L; Scheidegger, 1973) extended by a dataset of Li (1983). The rock avalanche of Molveno is marked with a red star. The inset shows the definition of the fall height (H) and runout length (L).

point, the model changes from simulating frictional sliding of a rigid body to simulating a granular flow with the Voellmy rheology. At 60 s the landslide collides with the opposite valley, and spreads to the North and the South. This symmetrical spreading is not expected from field mapping, it is explained though by the large depression which was created at the location of present-day Lago di Molveno (see section "Reconstruction of pre-failure topography and volume analysis"). At t = 90 s the landslide mass starts to flow back from the eastern flank and has reached its maximum extent in the North, albeit not in the South. At around t = 120 s (**Figure 8**) the model has reached its maximum extent.

The maximum velocity of the slide is reached at 30 s, when the movement changes from rigid, frictional sliding to granular flow with a Voellmy rheology. The maximum modeled velocity as the mass crosses the valley floor is 90 m/s, comparably estimated as 83 m/s from field-observed runup on the opposing valley flank [using $v = \sqrt{2gh}$ (Fahnestock, 1978)]. Reported rock avalanche velocities range from about 42 to 150 m/s (Heim, 1932; Evans et al., 1994). The modeled run-up reaches up to 550 m above the reconstructed valley floor to around 1250 m a.s.l. This indicates that the modeled run-up at one location just south of Pian delle Gaorne, where the highest run-up was modeled (**Figure 9**), might be slightly overestimated.

The runout model well reproduced the extent of the landslide, with the exception of the northern part. The deposit thickness was reproduced reasonably well except in Pian delle Gaorne and Moline, where the simulated deposit is too thin (**Figures 9**, **10B**). There are several possible reasons for this: (1) Uncertainties in the pre-failure topography, as the highest difference between

TABLE 4 | Properties of path-materials for the best-fit model run.

	Sliding plane (source zone)	Disintegrated mass movement (deposition zone)
Rheology	Frictional	Voellmy
Unit weight (kN/m^3)	20	20
Friction angle (°)	12	–
Pore pressure coeff. (R_u; –)	0	–
Friction coefficient μ (–)	–	0.2
Turbulence coefficient ξ (m/s^2)	–	500
Internal friction angle (°)	35	35

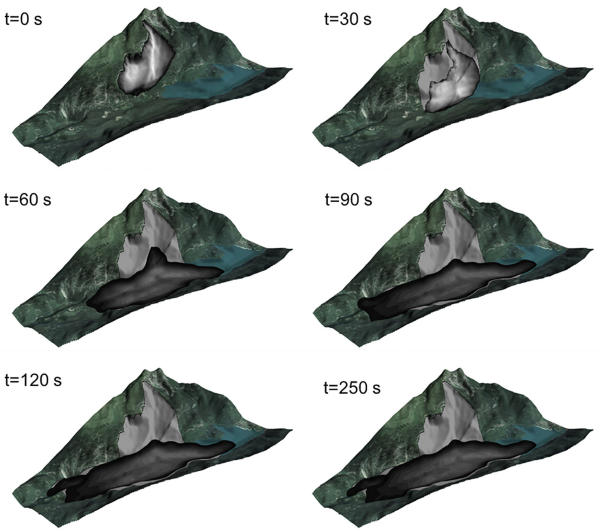

FIGURE 8 | Time series of runout. The first image at t = 0 s is showing the initial state. The first 30 s are in flexible mode that means the whole mass moves as intact body with a frictional rheology. After t = 30 s the model disintegrates and behaves as a Voellmy liquid. At t = 60 s the model runs up on Monte Gazza (opposite side of valley). At t = 90 s the model spreads more to *N* and *S*. At this time the landslide material already flowed back down from Monte Gazza. The gray colored area shows its maximum extent. At t = 120 s the maximum extent of the model is reached and only small changes in thickness and internal movement still happen. Photo by AGEA© 2011.

estimated and modeled thickness occurs on Pian delle Gaorne and the southern parts of the deposits where no seismic data were available. (2) Limitations of the numerical model, as the numerical technique used cannot simulate internal collapses where steep ridges are formed. This could potentially explain why the highest uncertainties lay in areas where the deposit creates steep ridges and deep depressions (Compare **Figure 10B** with **Figures 2A,B**). The calibrated parameters, shown in **Table 4**, are comparable with similar case studies (Aaron and McDougall, 2019).

The chosen friction angle of 12° for modeling the slide in the source area is low, however, it was well constrained by the absence of deposition in the source zone and matches values presented by Aaron and McDougall (2019). Cruden and Krahn (1978) measured ultimate friction angles as low as 14° along flexural slip planes found in the debris of the Frank slide, which had an approximate volume of 36.5 Mm^3. Aaron and McDougall (2019) showed with Dan3D modeling of a series of rock avalanches that friction angles of the sliding plane are inversely correlated with the volume of the slide. This may be related to breakage of asperities and extreme polishing of the sliding plane, which leads to a reduction of the friction angle to an ultimate friction angle (Cruden and Krahn, 1978). This process is dependent on normal stress and hence on the thickness of the sliding mass. Since the volume of the Molveno rock avalanche was significantly higher than volume of the Frank slide, an ultimate friction angle below 14° seems to be possible.

DISCUSSION

The combination of geomorphic mapping, runout modeling, and cosmogenic nuclide dating suggests that the Molveno rock avalanche occurred as one event, with the potential exception of the deposits at Nembia. Thus, the prominent internal scarps (**Figure 2**) must result from dynamic emplacement processes and do not provide evidence that the deposit is composed of multiple events. As shown on **Figure 8**, these features could be the result of extension of the moving debris along the irregular topography of the valley floor.

Our analysis has revealed several important preconditioning, preparatory, triggering, and emplacement factors that contributed to the Molveno rock avalanche (for a definition of these terms see McColl, 2012). The key preconditioning factors for the failure are the structural setting and the presence of marly interbeds with relatively weaker geotechnical properties. Lateral control of slope failure was along NW-SE oriented fractures that lie parallel to the Schio-Vicenza system (**Figure 1**). The basal rupture planes in both source niches are parallel to bedding, which has a mean dip angle of 23°(Castellarin et al., 2005a). Additionally, laboratory tests by Chinaglia and Fornero (1995) on the marly interbeds resulted in friction angles of approximately 25°. Thus, the slope was likely stable due to the presence of rock bridges.

Preparatory factors include glacial erosion, which steepened the valley and undercut the toe of the slope. This would have exposed the basal rupture plane, and likely contributed to time dependent strength degradation (e.g., Grämiger et al., 2017). However, the Molveno rock avalanche occurred 12,000 years after the valley was deglaciated, which suggests that other factors in addition to glacial debuttressing must have contributed to failure at this site. Heavy rain storms and wet climate in general have been suggested to be a possible trigger and driving factor for rock avalanches (Zerathe et al., 2014). Zerathe et al. (2014) found that many large landslides in the Western Alps are temporally related to a climatic period of high precipitation rates, with its peak at 4.2 ka. For the Austrian Alps a similar trend of landslides coinciding with a wetter period around the middle to late Holocene transition has been observed (Prager et al., 2008). Cycling of pore-water pressure due to frequent filling and draining of joints in the rock contributes to micro crack propagation and weakening of the rock mass (Gischig et al., 2016; Loew et al., 2017). Thus, heavy precipitation events or pore pressure changes due to seasonal climatic variations were likely an important preparatory factor for the Molveno rock avalanche (Gischig et al., 2016).

The trigger of the landslide could not be definitively constrained, however, the study area is known to be seismically active. Moderate earthquakes of magnitudes <6.0 have been documented (Basili et al., 2008), which are related to activity along the Giudicarie and the Schio-Vicenza fault systems (Viganò et al., 2013; Viganò et al., 2015). Dominant compression takes place along the Giudicarie and the Belluno–Bassano–Montello thrusts (Viganò et al., 2015). Strain is partitioned along the dominant right-lateral strike-slip faults of the Schio-Vicenza fault system (Viganò et al., 2015).

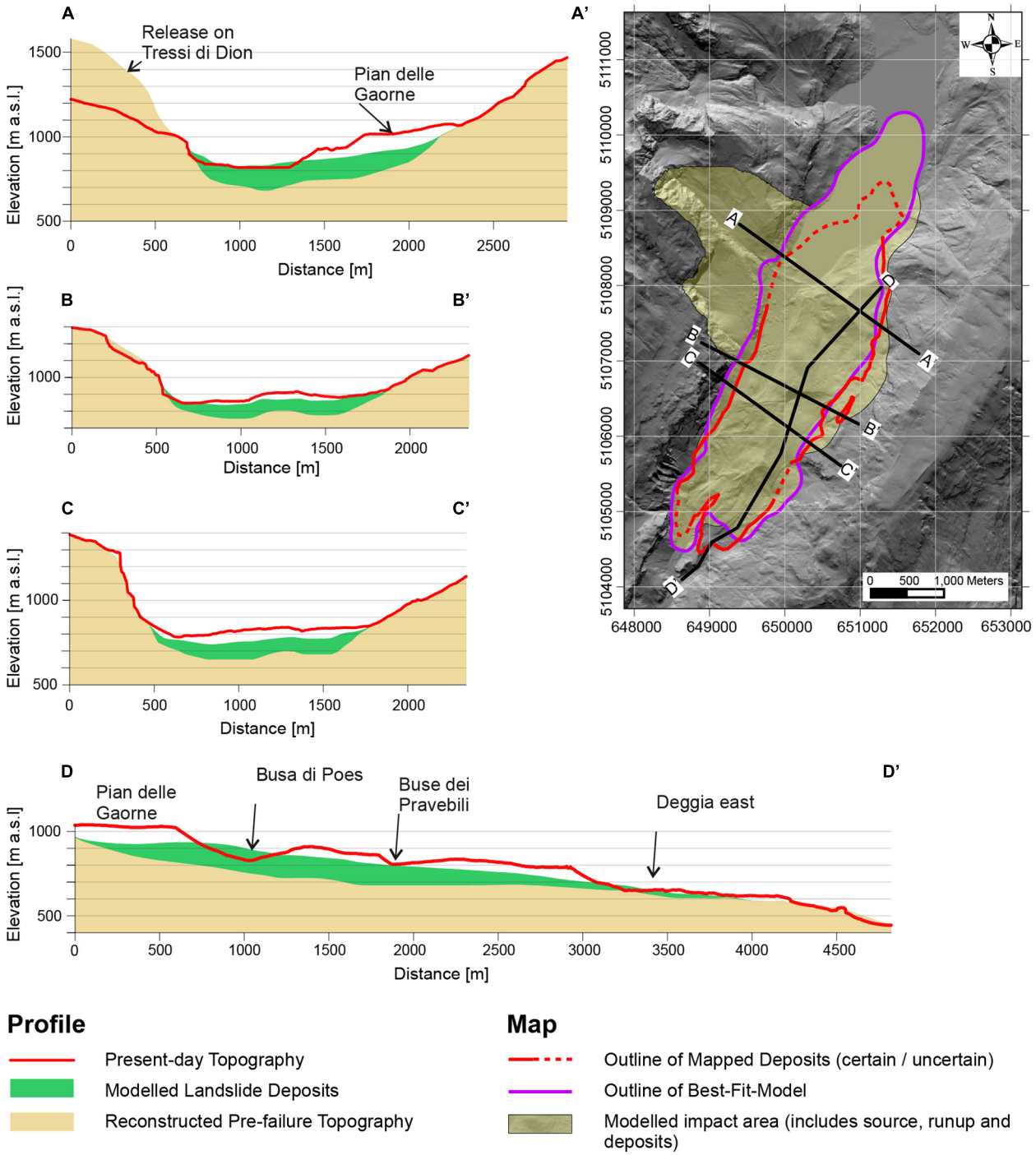

FIGURE 9 | Runout extent and thickness of modeled deposits. Best-fit model run. The modeled run-up on the eastern side could reproduce the mapped deposits and seems hence realistic. The southern margin is also quite well matched, except for the farther end of Deggia East. In the North the runout is too long into the lake. The thickness of the deposits does not match the estimated thickness of the pre-failure topography. Especially the thick deposit at Pian delle Gaorne cannot be reproduced.

A seismic trigger was also suggested for the nearby rock avalanches of Dro, Marocca Principale (5.3 ± 0.9 ka), and Kas (1.1 ± 0.2 ka; Ivy-Ochs et al., 2017a). As Marocca Principale is not only geographically close to Molveno but is also of the same age, within the uncertainties, a common seismic trigger is possible.

By combining geomorphic mapping, runout modeling and cosmogenic nuclide surface exposure dating, we can infer key

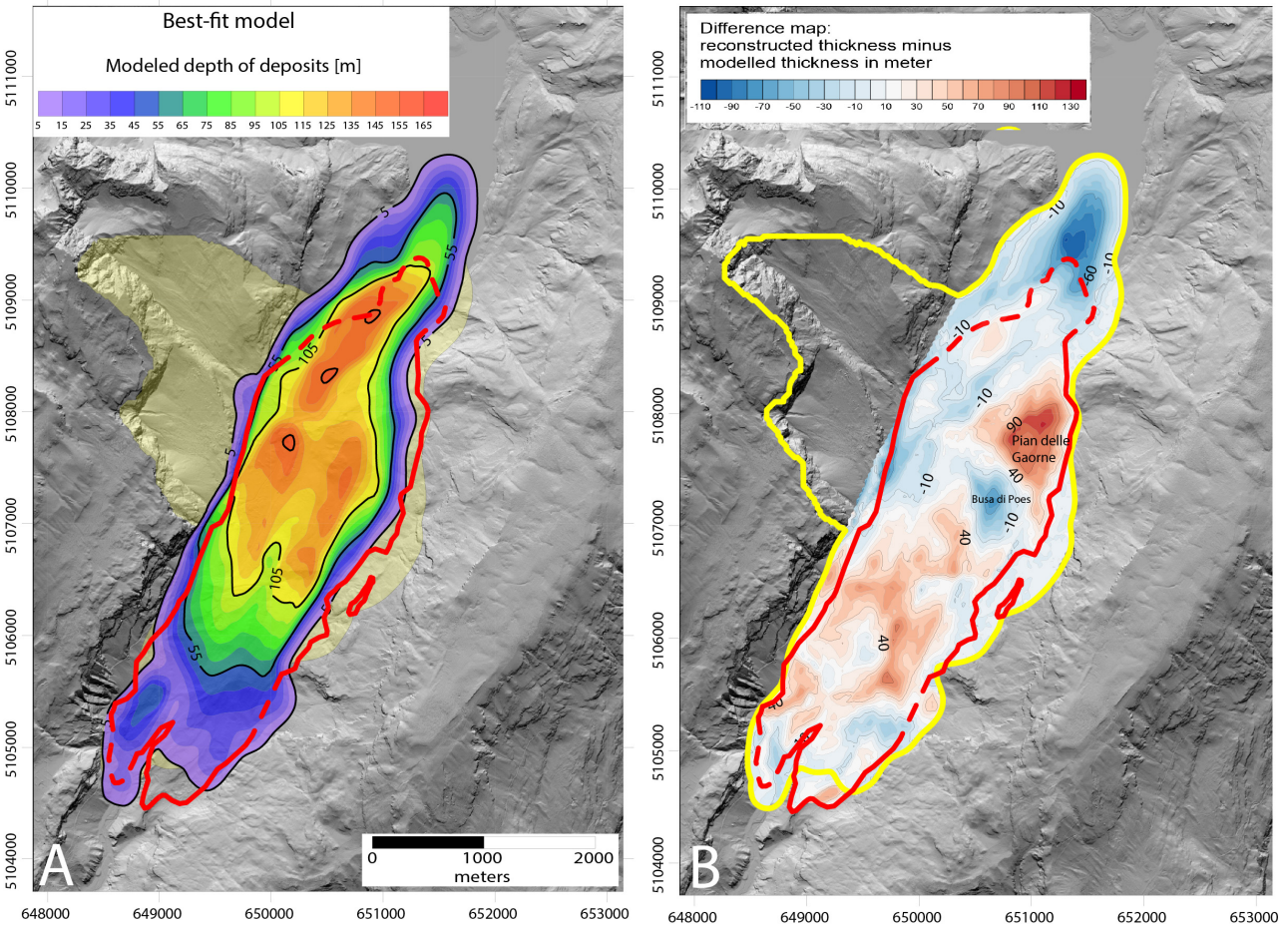

FIGURE 10 | (A) Depth map of the modeled deposits of the best-fit model. Contour interval is 10 m for the minor contour-lines and 50 m for the major contour-lines. The maximum impact area is marked in a pale yellow and the mapped landslide deposit is marked with a thick, red line. **(B)** Depth-difference-map between the estimated thickness when constructing the pre-failure topography and the modeled thickness of the best-fit model. The yellow outline indicates simulation results, and red indicates the mapped landslide deposits.

features regarding the dynamic characteristics of the Molveno rock avalanche. Dating suggests, that with the exception of Nembia (discussed above), all the deposit zones were emplaced simultaneously (at least within the uncertainties of the technique). Therefore, it is likely that the geomorphological features we mapped are evidence of dynamic runout processes. In Pian delle Gaorne, the inferred orientation of the direction of motion based on lineaments is different than the other zones except Buse dei Pravebili. This is consistent with direction of motion simulated by Dan3D-Flex, as runup and fallback are simulated in this area. Additionally, in Buse dei Pravebili, minor runup is also simulated, consistent with the rotated primary direction of the observed lineaments. In our simulations, strong depth gradients drive spreading along the valley, consistent with extensional features observed in the deposit. Finally, fall back ridges, similar to those observed at the Avalanche Lake Rock Avalanche (Aaron and Hungr, 2016a), can be seen in the areas of our simulated runup and fall back (**Figure 8**).

CONCLUSION

By combining cosmogenic ^{36}Cl exposure dating, detailed geomorphological mapping, volume reconstruction and numerical runout modeling, the constraints on the age and source area of the Molveno rock avalanche have been reconstructed. Cosmogenic ^{36}Cl dating combined with geomorphological mapping has shown that the main deposits are of the same age (4.8 $\pm$ 0.5 ka), with the exception of the deposits at Nembia, which have an age of 2.2 $\pm$ 0.2 ka. We speculate that in the Nembia area a lake of more than 10 m depth covered the deposits leading to the younger exposure dates. The age of the main event fits well within the middle Holocene peak in landslide activity, centering at 4.2 ka reported by other authors, and overlaps with the timing of the nearby Marocca Principale rock avalanche, within the dating uncertainties. Our geomorphic interpretation, confirmed by runout modeling, is that the landslide source area is located on Monte Soran, and that

the many scarps, lineaments and ridges in the deposit occurred during rock avalanche emplacement.

DATA AVAILABILITY STATEMENT

All datasets presented in this study are available upon reasonable request.

AUTHOR CONTRIBUTIONS

JW performed the field work, laboratory analysis, numerical modeling and interpretation, and assisted with the writing. SI-O conceived of the study, and performed the field work, laboratory analysis, data interpretation and assisted with the writing of the manuscript. JA assisted with the numerical modeling and data interpretation and assisted with the writing of the manuscript. SM conceived of the study, assisted with field work and data interpretation, and assisted with the writing of the manuscript. KL assisted with numerical modeling, data interpretation, and writing the manuscript. MR assisted with field work and data interpretation, and assisted with the writing of the manuscript. CV performed laboratory analysis, data interpretation and assisted with the writing of the manuscript. PC provided data used in the study, assisted with the field work and data interpretation, and assisted with writing the manuscript. AV provided data, assisted with field work and interpretation, an assisted with writing

FUNDING

This project was in part funded by the Geological Survey of Trento Province and the University of Padova (Progetto di ricerca di Ateneo 2014 and CPDA140511).

ACKNOWLEDGMENTS

The Geological Survey of Trento Province kindly provided access to the DEM. We appreciate support of fieldwork, laboratory work and AMS measurements by the Laboratory of Ion Beam Physics, ETH Zürich. Comments from two reviewers substantially improved the manuscript.

REFERENCES

Aaron, J., and Hungr, O. (2016a). Dynamic analysis of an extraordinarily mobile rock avalanche in the Northwest Territories, Canada. *Can. Geotech. J.* 53, 899–908. doi: 10.1139/cgj-2015-0371

Aaron, J., and Hungr, O. (2016b). Dynamic simulation of the motion of partially-coherent landslides. *Eng. Geol.* 205, 1–11. doi: 10.1016/j.enggeo.2016.02.006

Aaron, J., and McDougall, S. (2019). Rock avalanche mobility: the role of path material. *Eng. Geol.* 257, 105126. doi: 10.1016/j.enggeo.2019.05.003

Abele, G. (1974). *Bergstürze in den Alpen: ihre Verbreitung, Morphologie und Folgeerscheinungen*. Ph.D. thesis, Universität Karlsruhe, Karlsruhe.

Alfimov, V., and Ivy-Ochs, S. (2009). How well do we understand production of 36Cl in limestone and dolomite? *Quat. Geochronol.* 4, 462–474. doi: 10.1016/j.quageo.2009.08.005

Balco, G., Stone, J. O., Lifton, N. A., and Dunai, T. J. (2008). A complete and easily accesible means of calculating surface exposure ages or erosion rates from 10Be and 26Al measurements. *Quat. Geochronol.* 3, 174–195.

Basili, R., Valensise, G., Vannoli, P., Burrato, P., Fracassi, U., Mariano, S., et al. (2008). The Database of Individual Seismogenic Sources (DISS), version 3: Summarizing 20 years of research on Italy's earthquake geology. *Tectonophysics* 453, 20–43. doi: 10.1016/j.tecto.2007.04.014

Bigot-Cormier, F., Braucher, R., Bourlès, D., Guglielmi, Y., Dubar, M., and Stéphan, J. F. (2005). Chronological constraints on processes leading to large active landslides. *Earth Planet. Sci. Lett.* 235, 141–150. doi: 10.1016/j.epsl.2005.03.012

Carton, A. (2017). "Large ancient landslides in trentino, northeastern alps, as evidence of postglacial dynamics," in *Landscapes and Landforms of Italy*, eds M. Soldati, and M. Marchetti, (Padua: Springer International Publishing AG).

Castellarin, A., Dal Piaz, G. V., Picotti, V., Selli, L., Cantelli, L., Martin, S., et al. (2005a). *Carta Geologica D'Italia - Tione di Trento - Foglio 59, 1:50000*. Firenze: APAT.

Castellarin, A., Dal Piaz, G. V., Picotti, V., Selli, L., Cantelli, L., Martin, S., et al. (eds) (2005b). *Note illustrative della carta geologica d'Italia, Foglio n. 059, Tione di Trento*. Firenze: APAT.

Castellarin, A., Vai, G. B., and Cantelli, L. (2006). The alpine evolution of the Southern Alps around the Giudicarie faults: a late cretaceous to early Eocene transfer zone. *Tectonophysics* 414, 203–223. doi: 10.1016/j.tecto.2005.10.019

Chinaglia, N. (1992). Le "Marocche" Della Bassa Valle del Sarca: scivolamenti Planari in unità calcaree stratificate. *I Conv. Naz. Giov. Ric. Geol. Appl.* 3, 47–56.

Chinaglia, N., and Fornero, E. (1995). Ipotesi sulla possibile evoluzione cinematica di un movimento profondo di versante: L'esempio del M. *Soran (Trentino meridionale)*. *Mem. Soc. Geol. Ital.* 50, 101–108.

Coe, J. A., Bessette-Kirton, E. K., and Geertsema, M. (2018). Increasing rock-avalanche size and mobility in Glacier Bay National Park and Preserve, Alaska detected from 1984 to 2016 Landsat imagery. *Landslides* 15, 393–407. doi: 10.1007/s10346-017-0879-7

Cossart, E., Braucher, R., Fort, M., Bourlès, D. L., and Carcaillet, J. (2008). Slope instability in relation to glacial debuttressing in alpine areas (Upper Durance catchment, southeastern France): evidence from field data and 10Be cosmic ray exposure ages. *Geomorphology* 95, 3–26. doi: 10.1016/j.geomorph.2006.12.022

Cruden, D., and Krahn, J. (1978). "Frank Rockslide, Alberta, Canada," in *Rockslides and Avalanches, Vol 1 Natural Phenomena*, ed. B. Voight, (Amsterdam: Elsevier Scientific Publishing), 97–112.

Damian, J. (1890). Der Molvenosee in Tirol. *Petermann. Mitt.* 36, 262–270.

Dufresne, A., and Davies, T. R. (2009). Longitudinal ridges in mass movement deposits. *Geomorphology* 105, 171–118.

Dufresne, A., Prager, C., and Bösmeier, A. (2016). Insights into rock avalanche emplacement processes from detailed morpho-lithological studies of the Tschirgant deposit (Tyrol. Austria). *Earth Surf. Process. Landforms* 41, 587–602. doi: 10.1002/esp.3847

Dunning, S. A. (2004). *Rock Avalanches in High Mountains*. Ph.D. thesis, University of Bedfordshire, Luton.

Evans, S. G., Hermanns, R. L., Strom, A., and Scarascia-Mugnozza, G. (2011). *Natural and Artificial Rockslide Dams*. Berlin: Springer Science & Business Media.

Evans, S. G., Hungr, O., and Enegren, E. G. (1994). The Avalanche Lake rock avalanche, Mackenzie Mountains, Northwest Territories, Canada: description, dating, and dynamics. *Can. Geotech. J.* 31, 749–768. doi: 10.1139/t94-086

Fahnestock, R. K. (1978). "Chapter 5 - Little Tahoma Peak Rockfalls and avalanches, Mount Rainier, Washington, U.S.A," in *Developments in Geotechnical Engineering*, ed. B. Voight, (Amsterdam: Elsevier).

Ferretti, P., and Borsato, A. (2004). Geologia e geomorfologia della Valle e del Lago di Tovel. *Studi Trent. Sci. Nat. Acta Biol.* 81, 173–187.

Fort, M., Cossart, E., Deline, P., Dzikowski, M., Nicoud, G., Ravanel, L., et al. (2009). Geomorphic impacts of large and rapid mass movements: a review. *Géomorphologie* 15, 47–64.

Fuganti, A. (1969). Studio geologico di sei grandi frane di roccia nella regione Trentino-Alto Adige. *Mem. Mus. Trid. Sc. Nat.* 17, 1–72.

Gischig, V., Preisig, G., and Eberhardt, E. (2016). Numerical Investigation of Seismically Induced Rock Mass Fatigue as a Mechanism Contributing to the Progressive Failure of Deep-Seated Landslides. *Rock Mech. Rock Eng.* 49, 2457–2478. doi: 10.1007/s00603-015-0821-z

Grämiger, L. M., Moore, J. R., Gischig, V. S., Ivy-Ochs, S., and Loew, S. (2017). Beyond debuttressing: Mechanics of paraglacial rock slope damage during repeat glacial cycles. *J. Geophys. Res. Earth Surf.* 122, 1004–1036. doi: 10.1002/2016JF003967

Grämiger, L. M., Moore, J. R., Vockenhuber, C., Aaron, J., Hajdas, I., and Ivy-Ochs, S. (2016). Two early Holocene rock avalanches in the Bernese Alps (Rinderhorn, Switzerland). *Geomorphology* 268, 207–221. doi: 10.1016/j.geomorph.2016.06.008

Heim, A. (1932). *Bergsturz und Menschenleben*. Zürich: Frez&Wasmuth Verlag.

Hippolyte, J. C., Bourlès, D., Braucher, R., Carcaillet, J., Léanni, L., Arnold, M., et al. (2009). Cosmogenic 10Be dating of a sackung and its faulted rock glaciers, in the Alps of Savoy (France). *Geomorphology* 108, 312–320. doi: 10.1016/j.geomorph.2009.02.024

Hippolyte, J. C., Brocard, G., Tardy, M., Nicoud, G., Bourlès, D., Braucher, R., et al. (2006). The recent fault scarps of the Western Alps (France): Tectonic surface ruptures or gravitational sackung scarps? A combined mapping, geomorphic, levelling, and 10Be dating approach. *Tectonophysics* 418, 255–276. doi: 10.1016/j.tecto.2006.02.009

Hovius, N., Stark, C. P., and Allen, P. A. (1997). Sediment flux from a mountain belt derived by landslide mapping. *Geology* 25, 231–234.

Huggel, C., Allen, S., Clague, J. J., Fischer, L., Korup, O., and Schneider, D. (2013). "Detecting potential climate signals in large slope failures in cold mountain regions," in *Landslide Science and Practice*, eds C. Margottini, P. Canuti, and K. Sassa, (Heidelberg: Springer).

Hungr, O. (1995). A model for the runout analysis of rapid flow slides, debris flows, and avalanches. *Can. Geotech. J.* 32, 610–623. doi: 10.1139/t95-063

Hungr, O., and Evans, S. G. (2004). Entrainment of debris in rock avalanches: an analysis of a long run-out mechanism. *GSA Bull.* 116, 1240–1252. doi: 10.1130/b25362.1

Hungr, O., Evans, S. G., and Hazzard, J. (1999). Magnitude and frequency of rock falls and rock slides along the main transportation corridors of southwestern British Columbia. *Can. Geotech. J.* 224–238. doi: 10.1139/t98-106

Hungr, O., Leroueil, S., and Picarelli, L. (2014). The Varnes classification of landslide types, an update. *Landslides* 11, 167–194. doi: 10.1007/s10346-013-0436-y

Hungr, O., and McDougall, S. (2009). Two numerical models for landslide dynamic analysis. *Comput. Geosci.* 35, 978–992. doi: 10.1016/j.cageo.2007.12.003

Ivy-Ochs, S., and Kober, F. (2008). Surface exposure dating with cosmogenic nuclides. *Quat. Sci. J.* 57, 179–209.

Ivy-Ochs, S., Martin, S., Campedel, P., Hippe, K., Alfimov, V., Vockenhuber, C., et al. (2017a). Geomorphology and age of the Marocche di Dro rock avalanches (Trentino, Italy). *Quat. Sci. Rev.* 169, 188–205. doi: 10.1016/j.quascirev.2017.05.014

Ivy-Ochs, S., Martin, S., Campedell, P., Hippe, K., Vockenhuber, C., Carugati, G., et al. (2017b). "Geomorphology and age of large rock avalanches in Trentino (Italy): Castelpietra," in *Advancing Culture of Living with Landslides. WLF 2017*, eds M. Mikoš, V. Vilímek, Y. Yin, and K. Sassa, (Cham: Springer), doi: 10.1007/978-3-319-53483-1_41

Ivy-Ochs, S., Synal, H.-A., Roth, C., and Schaller, M. (2004). Initial results from isotope dilution for Cl and 36Cl measurements at the PSI/ETH Zurich AMS facility. *Nucl. Instrum. Methods Phys. Res. Sect. B* 22, 623–627. doi: 10.1016/j.nimb.2004.04.115

Kellerer-Pirklbauer, A., Lieb, G. K., Avian, M., and Carrivick, J. (2012). Climate change and rock fall events in high mountain areas: numerous and extensive rock falls in 2007 at Mittlerer Burgstall, Central Austria. *Geogr. Ann. Ser. A* 94, 59–78. doi: 10.1111/j.1468-0459.2011.00449.x

Knapp, S., Gilli, A., Anselmetti, F. S., Krautblatter, M., and Hajdas, I. (2018). Multistage rock-slope failures revealed in lake sediments in a seismically active Alpine region (Lake Oeschinen, Switzerland). *J. Geophys. Res. Earth Surf.* 123, 658–677. doi: 10.1029/2017JF004455

Köpfli, P., Grämiger, L. M., and Moore, J. R. (2018). The Oeschinensee rock avalanche, Bernese Alps, Switzerland: a co-seismic failure 2300 years ago? *Swiss J. Geosci.* 111, 205–219. doi: 10.1007/s00015-017-0293-0

Korup, O., and Clague, J. J. (2009). Natural hazards, extreme events, and mountain topography. *Quat. Sci. Rev.* 28, 977–990. doi: 10.1016/j.quascirev.2009.02.021

Korup, O., and Tweed, F. (2007). Ice, moraine, and landslide dams in mountainous terrain. *Quat. Sci. Rev.* 26, 3406–3422.

Kremer, K., Gassner-Stamm, G., Grolimund, R., Wirth, S. B., Strasser, M., and Fäh, D. (2020). A database of potential paleoseismic evidence in Switzerland. *J. Seismol.* doi: 10.1007/s10950-020-09908-5

Le Roux, O., Schwartz, S., Gamond, J. F., Jongmans, D., Bourles, D., Braucher, R., et al. (2009). CRE dating on the head scarp of a major landslide (Séchilienne, French Alps), age constraints on Holocene kinematics. *Earth Planet. Sci. Lett.* 280, 236–245. doi: 10.1016/j.epsl.2009.01.034

Lepsius, R. (1878). *Das Westliche Südtirol: Geologisch Dargest*. Berlin: W. Hertz.

Li, T. (1983). A mathematical model for predicting the extent of a major rockfall. *Z. Geomorphol.* 27:473482.

Loew, S., Gschwind, S., Gischig, V., Keller-Signer, A., and Valenti, G. (2017). Monitoring and early warning of the 2012 Preonzo catastrophic rocklope failure. *Landslides* 14, 141–154. doi: 10.1007/s10346-016-0701-y

Marchesoni, V. (1954). Il lago di Molveno e la foresta riaffiorata in seguito allo svaso. *Studi Trent. Sci. Nat.* 31, 9–24.

Marchesoni, V. (1958). La datazione col metodo del Carbonio 14 del lago di Molveno e dei resti vegetali riemersi in seguito allo svaso. *Studi Trent. Sci. Nat.* 2, 95–98.

Marrero, S. M., Phillips, F. M., Caffee, M. W., and Gosse, J. C. (2016). CRONUS-Earth cosmo-genic36Cl calibration. *Quat. Geochronol.* 31, 199–219. doi: 10.1016/j.quageo.2015.10.002

Martin, S., Campedel, P., Ivy-Ochs, S., Viganò, A., Alfimov, V., Vockenhuber, C., et al. (2014). Lavini di Marco (Trentino, Italy): 36Cl exposure dating of a polyphase rock avalanche. *Quat. Geochronol.* 19, 106–116. doi: 10.1016/j.quageo.2013.08.003

McColl, S. T. (2012). Paraglacial rock-slope stability. *Geomorphology* 153, 1–16. doi: 10.1016/j.geomorph.2012.02.015

McDougall, S., and Hungr, O. (2004). A model for the analysis of rapid landslide motion across three-dimensional terrain. *Can. Geotech. J.* 41, 1084–1097. doi: 10.1139/t04-052

Prager, C., Zangerl, C., Patzelt, G., and Brandner, R. (2008). Age distribution of fossil landslides in the Tyrol (Austria) and its surrounding areas. *Nat. Hazards Earth Syst. Sci.* 8, 377–407. doi: 10.5194/nhess-8-377-2008

Savage, S. B., and Hutter, K. (1989). The motion of a finite mass of granular material down a rough incline. *J. Fluid Mech.* 199, 177–215. doi: 10.1017/S0022112089000340

Scheidegger, A. E. (1973). On the prediction of the reach and velocity of catastrophic landslides. *Rock Mech.* 5, 231–236.

Schwinner, R. (1912). Der Mte. Spinale bei Campiglio und andere Bergstürze in den Südalpen. *Aust. J. Earth Sci.* 5, 127–197.

Singeisen, C., Ivy-Ochs, S., Wolter, A., Steinemann, O., Akçar, N., Yesilyurt, S., et al. (2020). The Kandersteg rock avalanche (Switzerland): integrated analysis of a late Holocene catastrophic event. *Landslides*. doi: 10.1007/s10346-020-01365-y

Steinemann, O., Ivy-Ochs, S., Grazioli, S., Luetscher, M., Fischer, U. H., Vockenhuber, C., et al. (2020). Quantifying glacial erosion on a limestone bed and the relevance for landscape development in the Alps. *Earth Surf. Process. Landforms*. 45, 1401–1417. doi: 10.1002/esp.4812

Stoffel, M., and Huggel, C. (2012). Effects of climate change on mass movements in mountain environments. *Prog. Phys. Geogr. Earth Environ.* 36, 421–439. doi: 10.1177/0309133312441010

Stone, J. O. H., Allan, G. L., Fifield, L. K., and Cresswell, R. G. (1996). Cosmogenic chlorine-36 from calcium spallation. *Geochim. Cosmochim. Acta* 60, 679–692. doi: 10.1016/0016-7037(95)00429-7

Strom, A. (2006). *Morphology and Internal Structure of rockslides and Rock Avalanches: Grounds and Constraints for their Modelling*. Dordrecht: Springer, 305–326.

Trener, G. B. (1906). Geologische aufnahme im nördlichen abhang der presanellagruppe. *J. K. K. Geol. Reichsanst.* 56, 405–496.

Trevisan, L. (1939). *Il Gruppo di Brenta:(Trentino occidentale)*. Rome: Istituto poligrafico dello Stato.

Vecchia, O. (1953). Recherches geophysiques pour un barrage au Lac de Molveno. *Riv. Geofisica Appl.* 14, 73–85.

Viganò, A., Scafidi, D., Martin, S., and Spallarossa, D. (2013). Structure and properties of the Adriatic crust in the central-eastern Southern Alps (Italy) from local earthquake tomography. *Terra Nova* 25, 504–512. doi: 10.1111/ter.12067

Viganò, A., Scafidi, D., Ranalli, G., Martin, S., Della Vedova, B., and Spallarossa, D. (2015). Earthquake relocations, crustal rheology, and active deformation in the central–eastern Alps (N Italy). *Tectonophysics* 661, 81–98. doi: 10.1016/j.tecto.2015.08.017

Vockenhuber, C., Miltenberger, K. U., and Synal, H. A. (2019). 36Cl measurements with a gas-filled magnet at 6 MV. *Nucl. Instrum. Methods Phys. Res. Sect. B* 455, 190–194. doi: 10.1016/j.nimb.2018.12.046

Weidinger, J. T., Korup, O., Munack, H., Altenberger, U., Dunning, S. A., Tippelt, G., et al. (2014). Giant rockslides from the inside. *Earth Planet. Sci. Lett.* 389, 62–73. doi: 10.1016/j.epsl.2013.12.017

Wolter, A., Stead, D., Ward, B. C., Clague, J. J., and Ghirotti, M. (2016). Engineering geomorphological characterisation of the Vajont Slide, Italy, and a new interpretation of the chronology and evolution of the landslide. *Landslides* 13, 1067–1081. doi: 10.1007/s10346-015-0668-0

Zerathe, S., Lebourg, T., Braucher, R., and Bourlès, D. (2014). Mid-Holocene cluster of large-scale landslides revealed in the Southwestern Alps by 36Cl dating. Insight on an Alpine-scale landslide activity. *Quat. Sci. Rev.* 90, 106–127. doi: 10.1016/j.quascirev.2014.02.015

Conflict of Interest: The authors declare that the research was conducted in the absence of any commercial or financial relationships that could be construed as a potential conflict of interest.